Hydraulic Tomography and the Impact of *A Priori* Information: An Alluvial Aquifer Example
(Kansas Geological Survey Open-file Report 2003-71)

By Geoffrey C. Bohling[1], Xiaoyong Zhan[1], Michael D. Knoll[2], and James J. Butler, Jr.[1]

[1] Kansas Geological Survey, University of Kansas
[2] Center for Geophysical Investigation of the Shallow Subsurface, Boise State University

Abstract

Hydraulic tomography is a recently developed aquifer characterization technique that involves the performance of a large number of short-term pumping tests, each of which stresses a different vertical interval in a well. Simultaneous analysis of drawdown measurements obtained from the entire set of tests provides the potential to estimate between-well hydraulic conductivity (K) variations at a higher level of detail than is possible with more conventional well tests. Hydraulic tomography is still plagued by the ubiquitous problem of non-uniqueness, so reasonable estimates of the K distribution are difficult to obtain without incorporating independent *a priori* information on aquifer structure. In this study, we investigate the utility of cross-hole radar surveys as a source of *a priori* information on the spatial structure of the K field. We compare the results of analyzing a suite of tomographic pumping tests performed in an extensively studied alluvial aquifer using regularly layered zonations and zonations derived from the results of zero-offset cross-hole radar profiles. In all cases, residuals between predicted and observed drawdowns, chi-squared values for the model fit, and K estimates obtained from direct-push slug tests are used as the basis for comparison. Radar-based approaches can potentially provide valuable information about K variations between wells due to the dependence of radar propagation velocity and attenuation on sediment porosity and clay content. This study demonstrates that electromagnetic and hydraulic properties at the study site seem to be governed at least to some extent by the same sediment variations, meaning that radar surveys are indeed capable of providing information regarding the K field geometry.

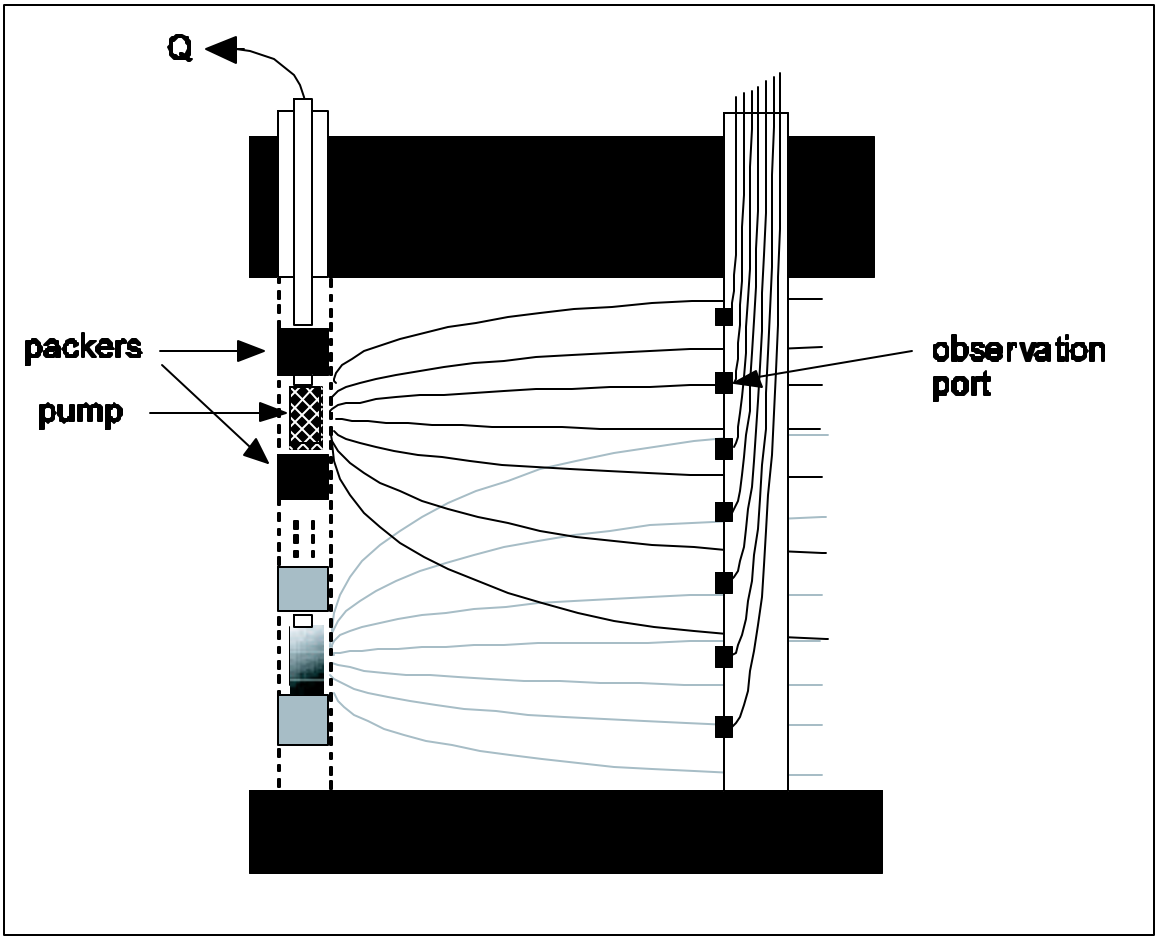

Figure 1. Schematic representation of two tests in a series of tomographic pumping tests.

Hydraulic Tomography Concept

Hydraulic tomography (Bohling *et al.*, 2002; Butler *et al.*, 1999; Yeh and Liu, 2000) involves performing a series of pumping tests stressing different vertical intervals in an aquifer with drawdowns measured at multiple observation points during each test (Figure 1). Simultaneous analysis of data from all the tests allows characterization of the hydraulic conductivity (K) distribution between wells at a higher resolution than is provided by more conventional aquifer testing methods.

Despite the high information density provided by the tomographic format, the estimation of hydraulic conductivity from the observed drawdowns is still plagued by the non-uniqueness that typifies parameter estimation problems in the earth sciences (Parker, 1994). Therefore, a reasonable zonation of the model aquifer is required to yield meaningful K estimates. In this study, we have used cross-hole ground-penetrating radar surveys to guide the flow model zonation, assuming that the hydraulic and electromagnetic property distributions are governed to some extent by the same sediment geometry.

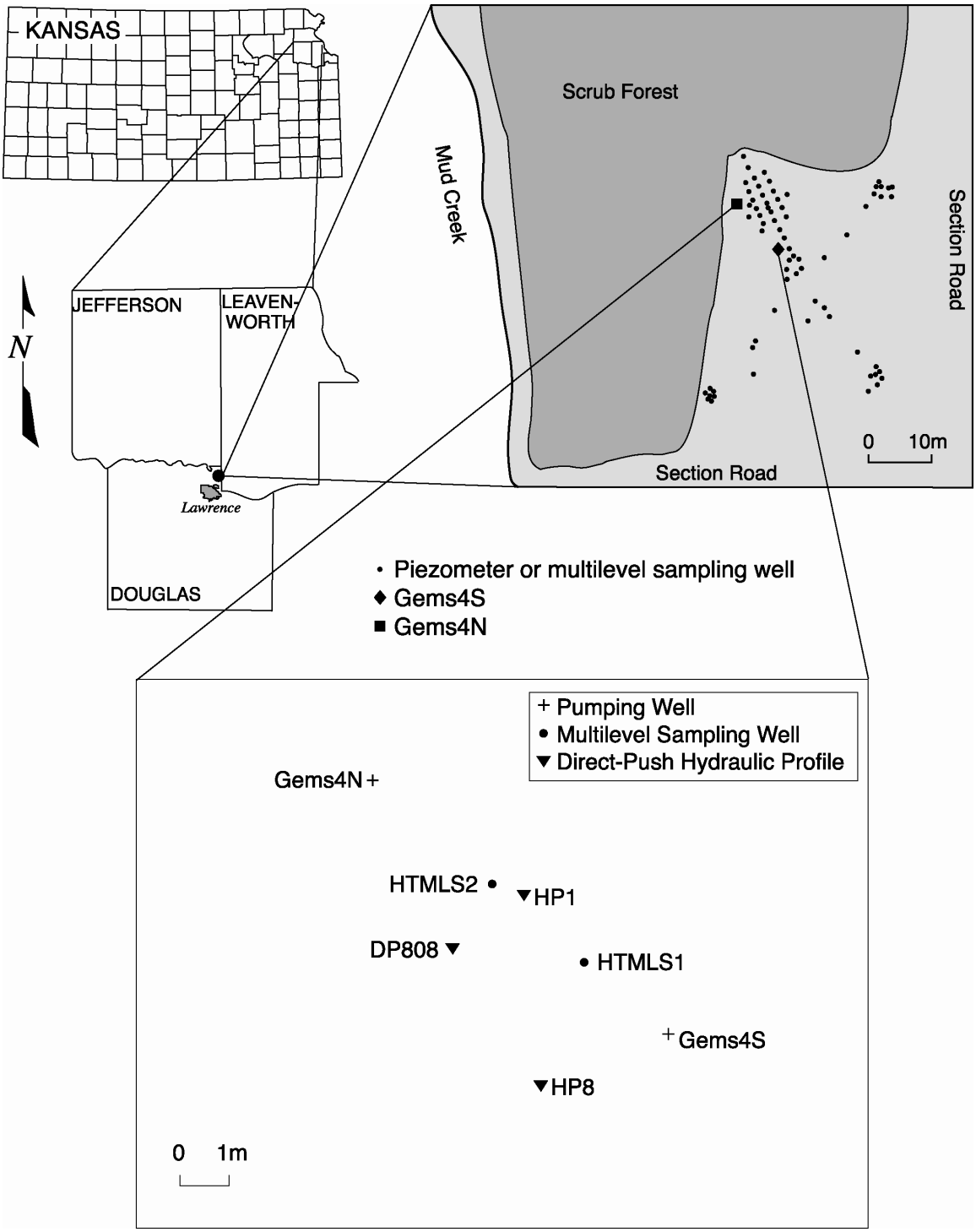

Figure 2. Location of site (GEMS) and wells used in current study. Scale in most expanded view is 1 meter.

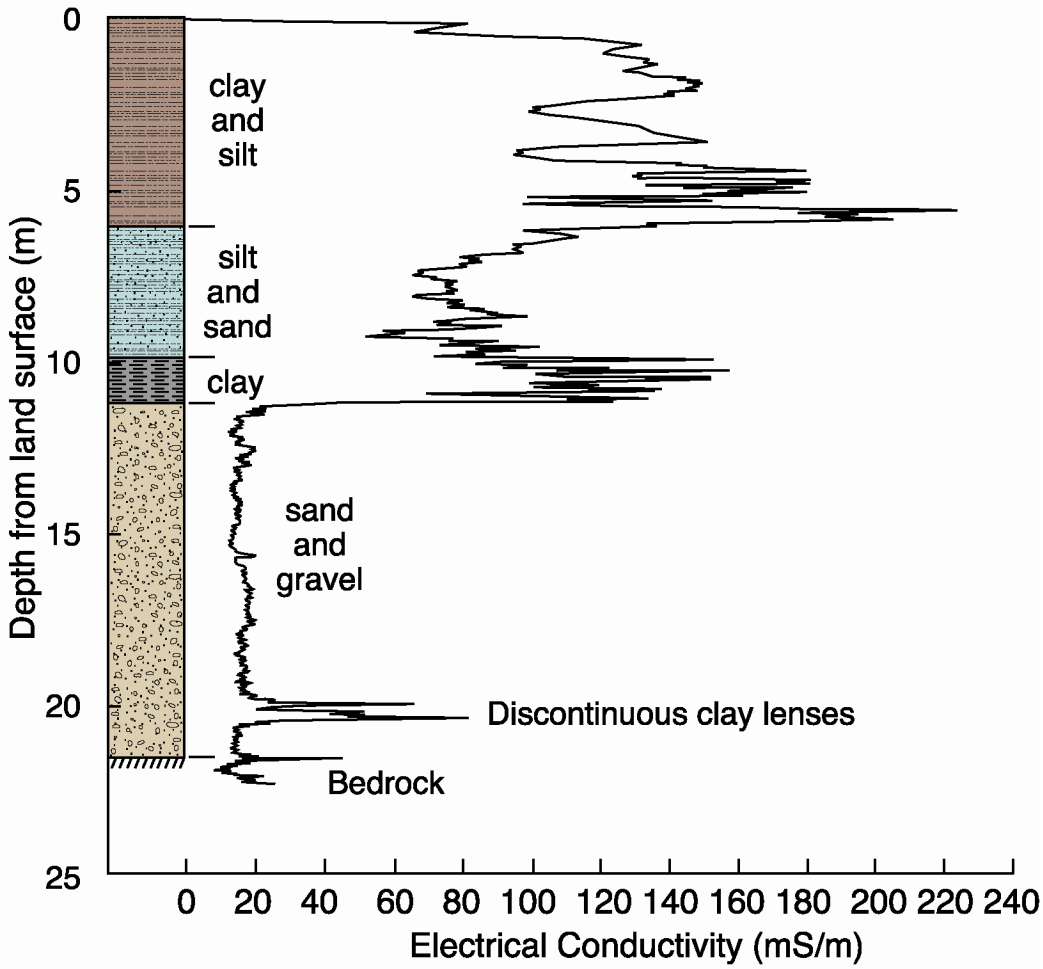

Figure 3. Sediment sequence at GEMS together with electrical conductivity profile.

Study Site

We have performed the hydraulic tomograpahy experiments at the Kansas Geological Survey's Geohydrologic Experimental and Monitoring Site (GEMS), a heavily instrumented site in the Kansas River Valley northeast of Lawrence, Kansas (Figure 2). The alluvial aquifer at the site consists of 11 meters of sand and gravel overlain by 11 meters of silt and clay. The sediment profile at the site is shown in Figure 3, together with an electrical conductivity profile obtained using a direct-push probe (Schulmeister et al., 2003).

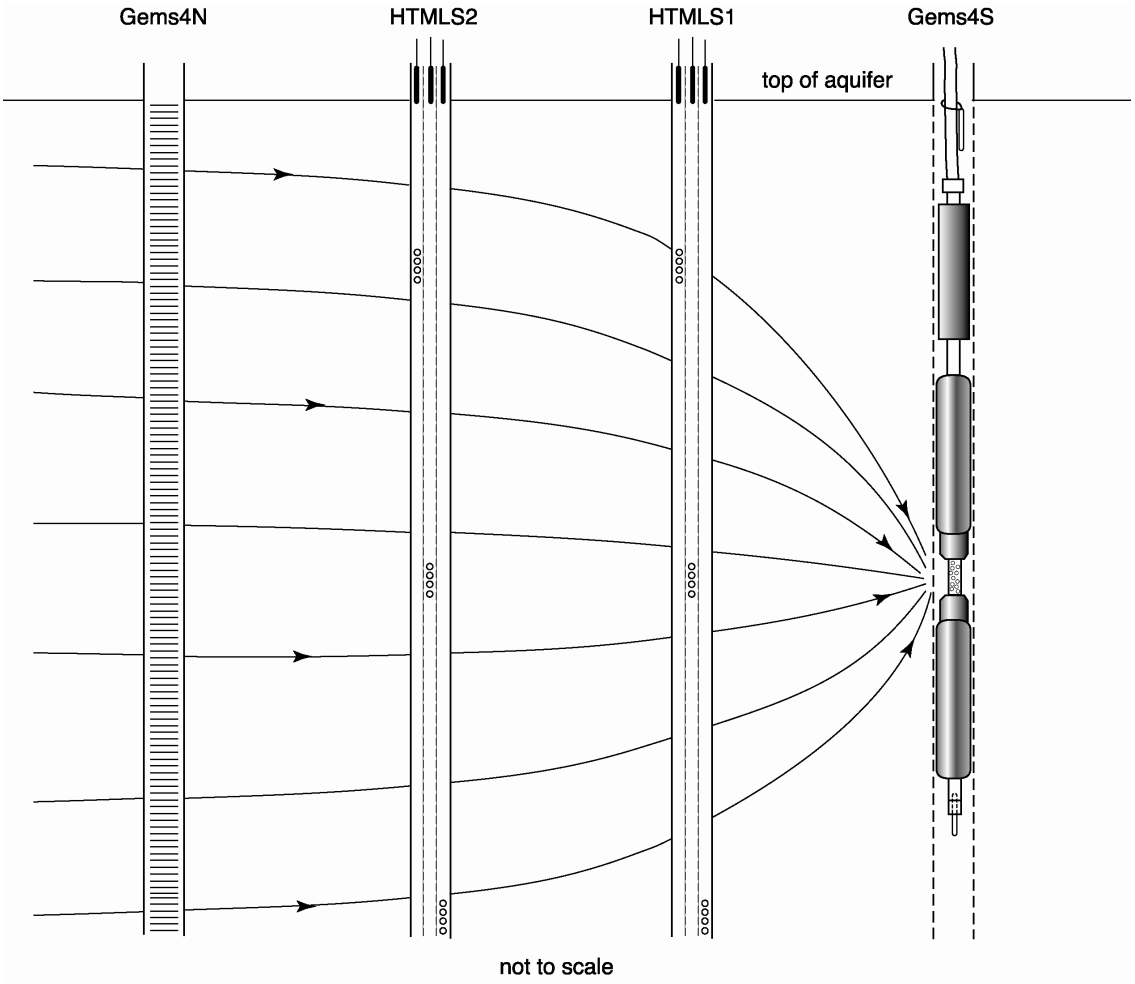

Figure 4. Experimental setup of tomographic pumping tests.

Experimental Setup

Gems4S was used as the pumping well for the hydraulic tomography experiments discussed here (Figure 4, Figure 2). Drawdowns were measured using pressure transducers installed in the observation wells HTMLS1 and HTMLS2. Each of these observation wells is made from 7-chamber PVC pipe with a screened opening in just one chamber at each sample depth. Changes in drawdown (pressure) at that depth are measured with a pressure transducer in the corresponding chamber.

In this study, we compare K estimates obtained from the tomographic pumping tests to estimates obtained from direct-push slug tests (Butler *et al.*, 2002; Sellwood *et al.*, 2001; McCall *et al.*, 2002) at the locations labeled HP1, HP8, and DP808 in Figure 2. Direct-push slug tests can provide accurate estimates of the hydraulic conductivity in the immediate vicinity of each testing point but do not yield definitive information on the connectivity of high- and low-conductivity zones. Hydraulic tomography, on the other hand, probes the material between wells, providing high-resolution information regarding potential contaminant transport pathways.

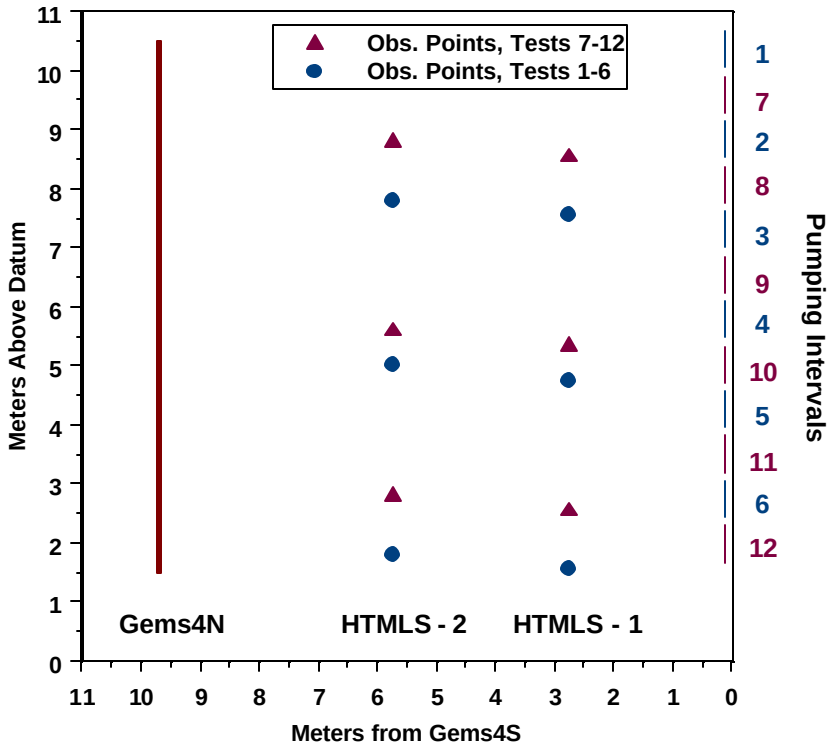

Figure 5. Pumping interval and observation point locations for 12 pumping tests.

Figure 5 shows the locations of the pumping intervals (in Gems4S) and observation points for the 12 tomographic pumping tests. Tests 1-6 were performed with increasing pumping interval depth, then the packer string was pulled back up and tests 7-12 were performed. Observations were obtained at six locations during each test, with three transducers installed in each of the two multilevel sampling wells. Between tests six and seven, the transducers were relocated (moved to different chambers), so that tests 7-12 used a different set of observation locations than tests 1-6.

Datum in Figure 5 corresponds roughly with the bottom of the aquifer and is taken as the bottom of the model aquifer. The model aquifer is 10.67 meters (35 feet) thick. The lack of observation points near the top of the aquifer and the lack of observation points and pumping intervals close to the bottom of the aquifer lead to poor resolution of the hydraulic conductivity in these regions.

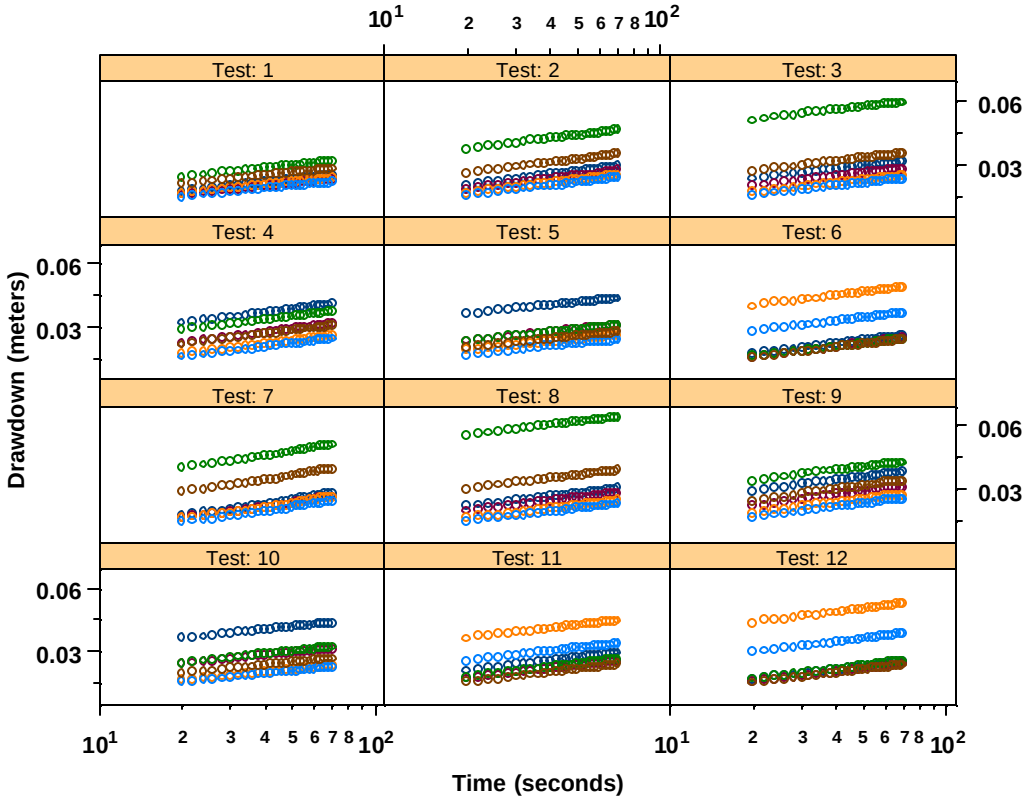

Figure 6. Drawdowns measured at six observation points (each represented by a different color) over all 12 tomographic pumping tests.

Steady-Shape Analysis of Drawdown Data

For each of the 12 tests, observed drawdowns from approximately 20 to 70 seconds following the initiation of pumping exhibit a fairly constant and common slope versus log-time along with constant drawdown differences between observation points. This behavior corresponds to a "steady-shape" drawdown configuration: gradients in the region of investigation are no longer changing, although drawdown is still increasing overall at a constant and common rate (Butler, 1988). Under steady-shape conditions, the slope of the drawdown versus log time plot is controlled by the bulk average horizontal hydraulic conductivity – Cooper-Jacob analyses of the 72 slopes shown in Figure 6 yield conductivity estimates centered around a mean of 130 meters/day with a standard deviation of 14 m/day – but the drawdown differences are controlled by the conductivity distribution in the region of investigation. In this case, the drawdown *differences* can be modeled and fit using steady-state simulations of the pumping tests, rather than transient simulations. This decreases computational time for the analyses by one to two orders of magnitude and also reduces the influence of poorly known boundary conditions (Bohling *et al.*, 2002).

For the analyses discussed here, the observations to be matched are the differences in drawdown between all 15 possible pairs of the six observation points for each of the 26 observation times (from 20 seconds to 70 seconds in two-second increments) for each test. That is, we essentially have 26 repeat measurements of each difference, since the differences are roughly constant over time. This leads to 390 observed drawdown differences per test, for a total of 4680 observations over all twelve tests.

To simulate and fit the data we have used a two-dimensional radial-vertical finite difference flow model coupled with the Levenberg-Marquardt nonlinear regression algorithm (Bohling and Butler, 2001). The flow model uses a logarithmically transformed radial coordinate given by $r' = \ln(r/r_w)$ where r is the actual radial distance from the center of the pumping well and r_w is the pumping well radius. This transformation allows radial flow to be simulated using a regular Cartesian (rectangular) grid. The model employed here uses 60 cells in the horizontal at a spacing of $\Delta r' = 0.2$ (dimensionless) and 70 cells in the vertical at a spacing of $\Delta z = 0.152$ m (0.5 feet). We also include an extra (zeroth) column of nodes to simulate the wellbore, with a combination of high- and low-conductivity cells representing the open wellbore and packer configuration for each test. This allows the model to incorporate the damping of vertical gradients that might result from bypass flow along the wellbore.

For this study we have used layered zonations of the model aquifer, with all cells in a given layer assigned a single hydraulic conductivity value. Tests are first run with equal-thickness layers and then with variable-thickness layers derived from interpretation of a zero-offset radar survey run between Gems4S and Gems4N, in the same vertical plane as the hydraulic tomography tests. A number of other zero-offset and tomographic radar surveys have also been performed at the site, but information from these surveys has not yet been incorporated into the flow modeling.

The nonlinear regression algorithm adjusts the hydraulic conductivity values for the different layers in an attempt to minimize a chi-squared objective function given by

$$c^2 = \sum_{i=1}^{n} \left[\left(dd_i^{obs} - dd_i^{prd} \right) / s_{dd} \right]^2$$

where n is the number of observations (4680), dd_i^{obs} is the i^{th} observed drawdown difference, dd_i^{prd} is the corresponding difference predicted by the model, and s_{dd} is the estimated measurement error (standard deviation) for the drawdown differences. Based on pressure transducer characteristics and on the residuals from the Cooper-Jacob analyses mentioned above, we have estimated the drawdown difference measurement error as $s_{dd} = 1 \times 10^{-4}$ m. This value is quite small relative to actual deviations between observed and predicted drawdown differences, leading to large c^2 values (highly significant lack of fit). However, the value is constant for all observations, so the estimated conductivity values are essentially the same as those that would be obtained from unweighted regression.

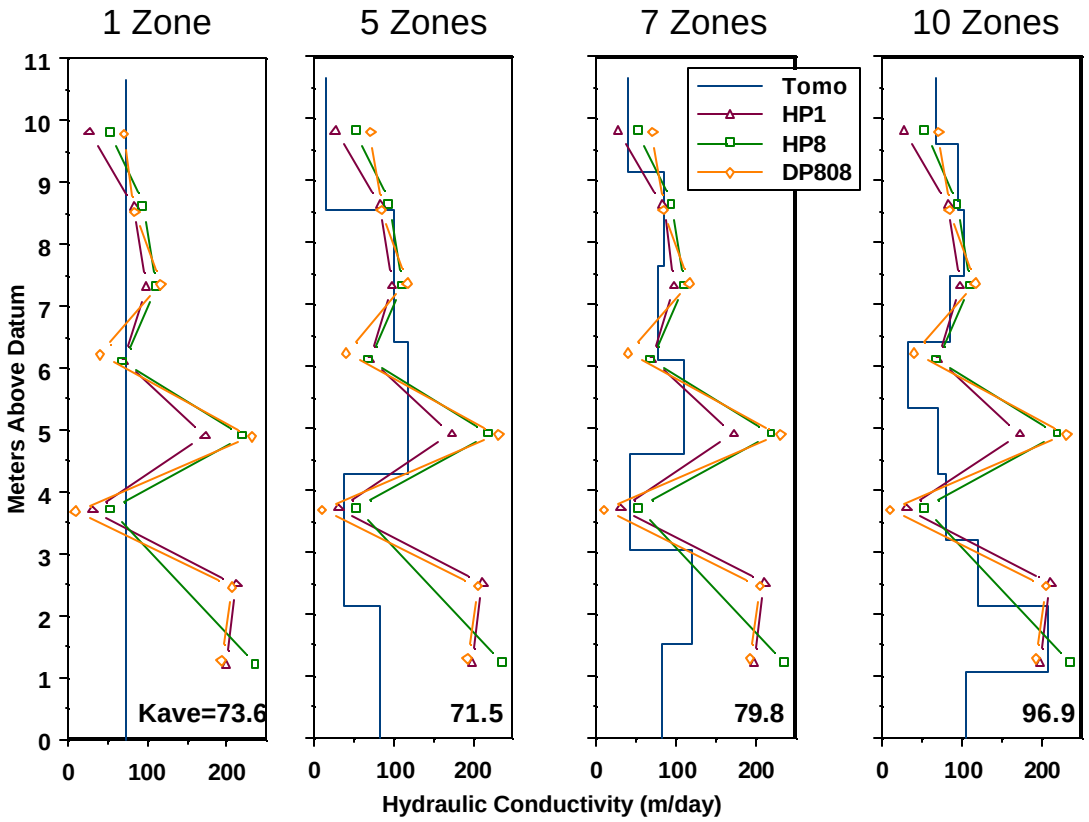

Figure 7. Estimated conductivities from hydraulic tomography (solid lines) with 1, 5, 7, and 10 equal-thickness zones (layers) compared to nearby direct-push slug test profiles.

Regular-Layer Zonations

Figure 7 shows the estimated hydraulic conductivity profiles obtained from steady-shape analysis of the drawdown differences using four different layered zonations, dividing the 10.67-meter (35-foot) thick aquifer into one, five, seven, and ten equal-thickness layers, respectively. These results are compared with conductivity estimates from direct-push slug test profiles at HP1, HP8, and DP808 (see map, Figure 2). The thickness-weighted average horizontal hydraulic conductivity (in m/day) for each case is shown at the bottom of each plot. These averages are clearly lower than the average of 130 m/day given by the Cooper-Jacob analyses and lower than the 116 m/day given by larger-scale pumping tests at the site. We believe that this discrepancy is due in part to undersampling of the high-conductivity region at the bottom of the aquifer in the tomographic pumping test suite (Figure 5). The tomography estimates compare reasonably well with the slug test results given the constraints of the imposed zonations, but we could clearly do a better job matching the aquifer geometry implied by the slug test profiles.

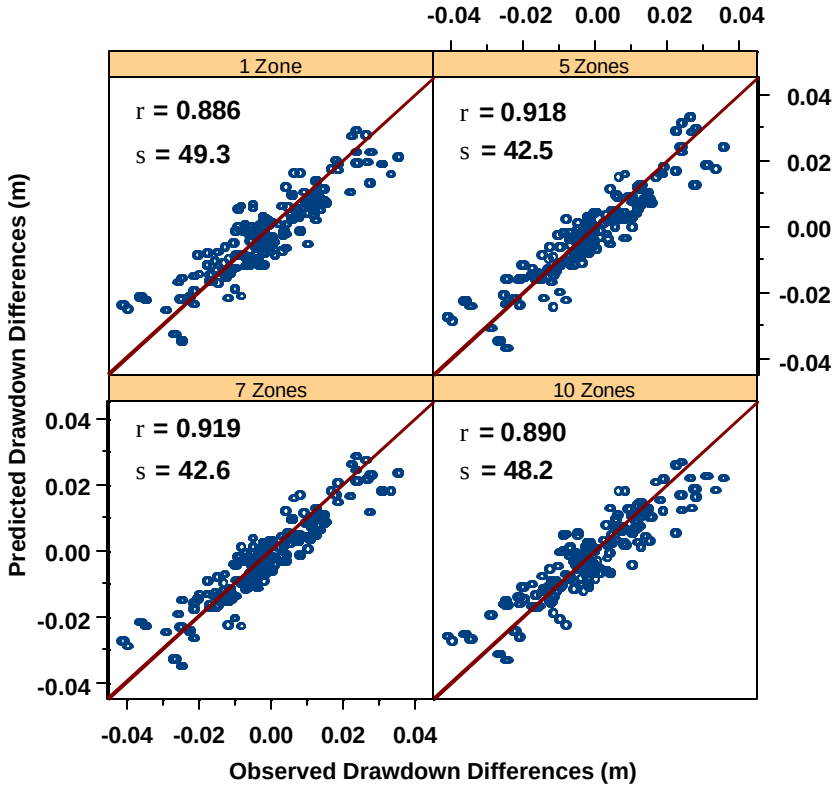

Figure 8. Predicted versus observed drawdown differences for equal-thickness zonations. ρ is the correlation between observed and predicted differences and σ is the root-mean-squared scaled residual for each fit.

Summary results for the regular-layer fits are shown in Figure 8. The root-mean-squared scaled residual shown is given by

$$s = \sqrt{c^2/df} = \sqrt{\left(\sum_{i=1}^{n}\left[\left(dd_i^{obs} - dd_i^{prd}\right)/s_{dd}\right]^2\right)/(n-p)}$$

where p is the number of estimated parameters (conductivity values) and $df = n - p$ represents the degrees of freedom for the fit. Because the actual residuals ($dd_i^{obs} - dd_i^{prd}$) are much larger than the estimated measurement error $s_{dd} = 1\times10^{-4}$ m, the root-mean-squared scaled residuals are quite large, meaning none of the models comes close to matching the data to within measurement error. It is possible that a larger value for s_{dd} would be more appropriate, taking into account more factors than just measurement error. The relative variations in s would be the same regardless of the choice of s_{dd}. In this case, the 5- and 7-layer zonations yield comparable fits, both notably better than the 1- and 10-zone fits. The fundamental question is whether we could do better using more informed zonations.

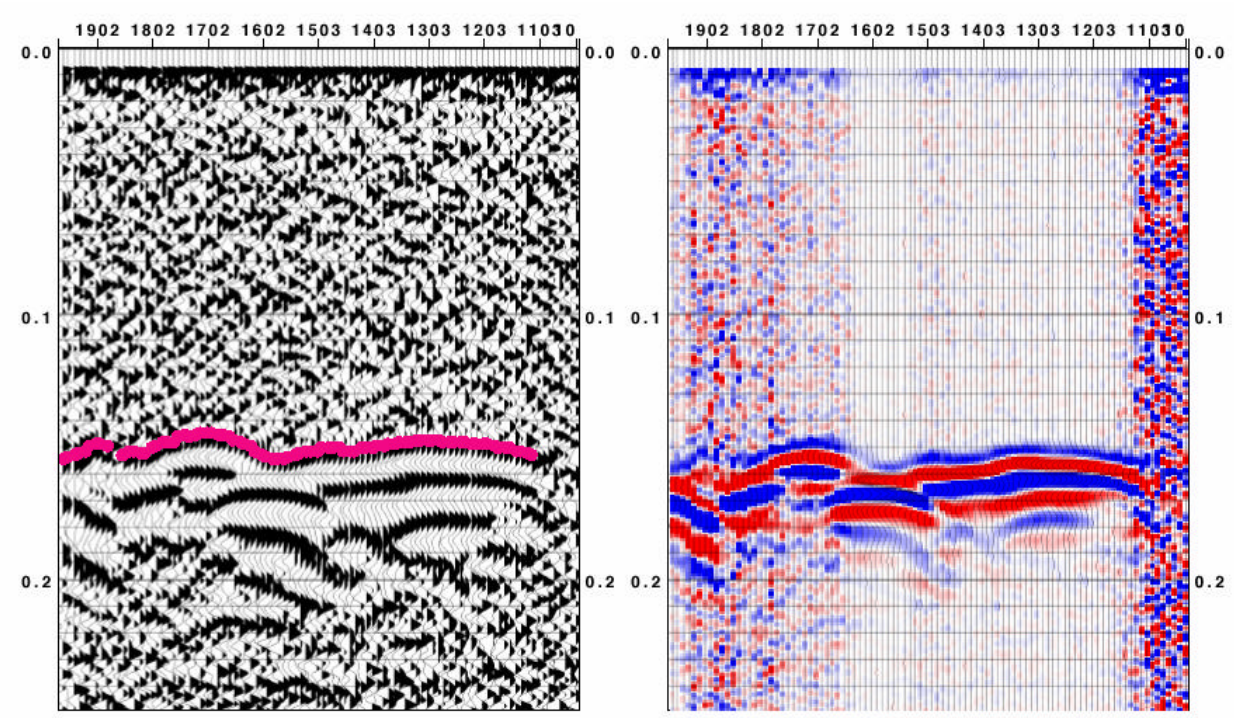

Figure 9. Zero-offset radar profile between Gems4S and Gems4N, shown as variable-gain wiggle traces (left) and color-coded amplitudes with no gain (right). Horizontal axis is depth below a datum at ground surface in centimeters, increasing to the left, and vertical axis is traveltime in microseconds. First-break picks are highlighted on left.

Interpretation of Zero-Offset Radar Profile

We will now investigate the utility of cross-hole radar surveys for guiding the zonation of the flow model. Figure 9 shows two different representations of a zero-offset radar profile run between Gems4S and Gems4N. These two wells are 10 meters apart and encompass the region tested by the hydraulic tomography experiments (Figure 2). This survey employed 100 MHz antennas, with the transmitting antenna in Gems4N and the receiving antenna in Gems4S. The two antennas were lowered together in 10-cm increments, thus remaining at approximately equal depths in the two wells. Figure 10 shows the propagation velocity and signal attenuation values derived from the first break travel times and peak amplitude variations, respectively. These values are plotted versus meters above datum for the flow model, together with zonal averages for a 13-layer interpretation of the data (Knoll, 2003), with layer boundaries adjusted to the nearest cell boundary in the flow model. In addition to using a zonation based on expert interpretation of the radar data, we were also interested in investigating zonations derived from more automated analysis. Figure 11 shows 5-, 7-, and 10-layer zonations derived from hierarchical depth-constrained cluster analysis (Gill *et al.*, 1993; Bohling *et al.*, 1998) of the velocity and attenuation values. The cluster analysis actually identified two additional thin layers in each case, including a 1-foot thick layer at the top of the aquifer, but these have been merged with adjacent layers due to the insensitivity of the flow model to the properties of these layers.

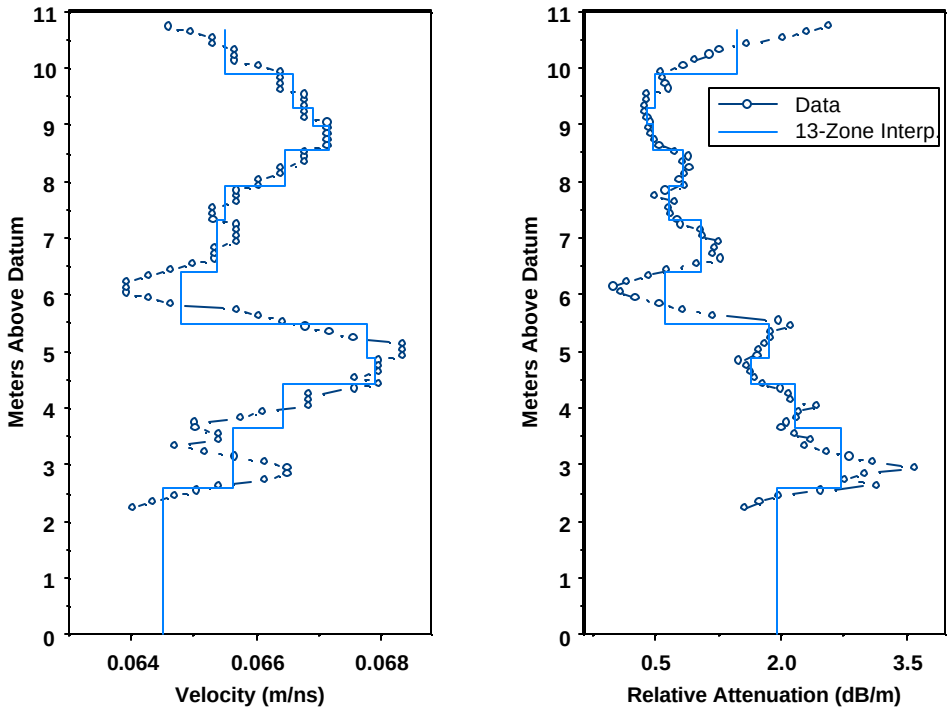

Figure 10. Radar velocity and attenuation values from zero-offset survey and expert interpretation of significant breaks (adjusted to nearest cell boundary in flow model).

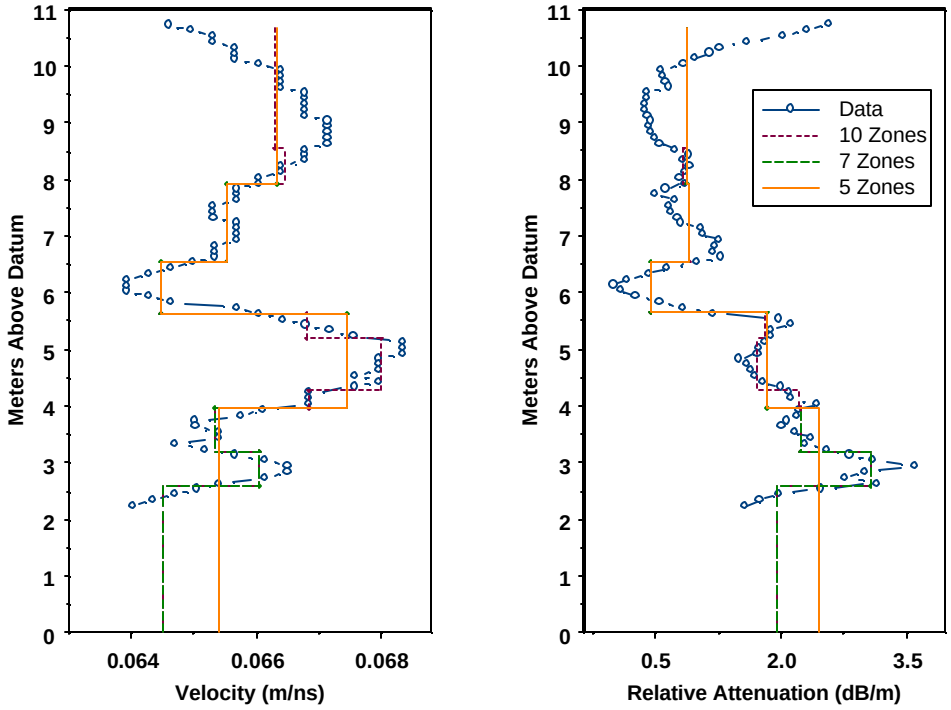

Figure 11. Automated zonations of velocity and attenuation data.

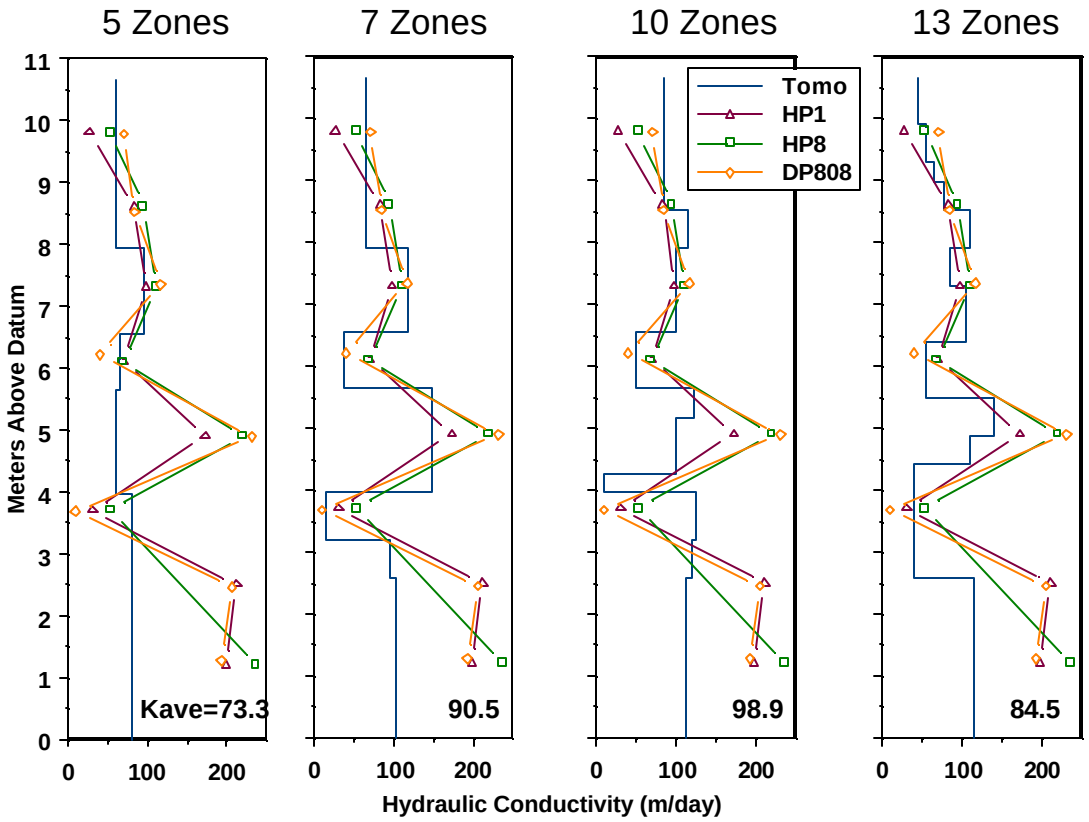

Figure 12. Estimated conductivities from hydraulic tomography (solid lines) using radar-based zonations compared to nearby direct-push slug test profiles.

Radar-Based Zonations

Figure 12 shows the estimated conductivity profiles using the radar-based zonations and Figure 13 shows the corresponding fit diagnostics. The seven-zone estimates show a remarkably good correspondence with the direct-push slug test profiles and also the best fit statistics overall, with a correlation of 0.936 between observed and predicted drawdown differences and a root-mean-squared scaled residual of $\sigma = 37.6$, notably better than all other fits (Table 1). Of the four radar-based zonations, the 13-layer expert zonation provides the most detail near the top of the aquifer and the agreement between the corresponding conductivity estimates and direct-push slug test results in this region is extremely good. These results give us some confidence that cross-hole radar surveys are capable of providing valuable information regarding the sediment variations controlling the distribution of hydraulic conductivity.

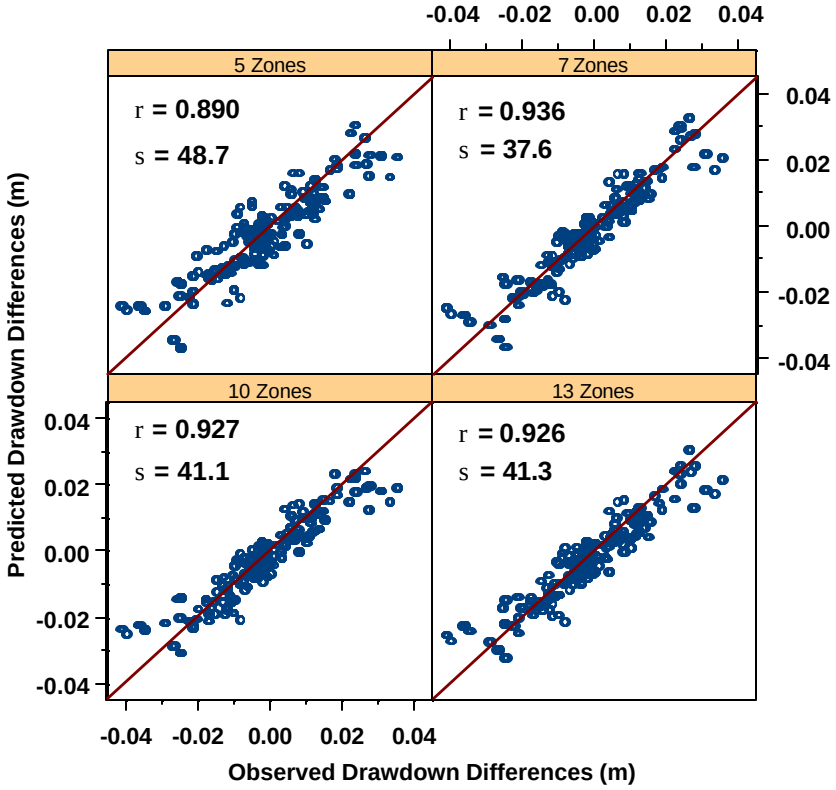

Figure 13. Predicted versus observed drawdown differences for radar-based zonations.

Zones	K_{ave}(m/d)	ρ	σ
1	73.6	.886	49.3
5 equal	71.5	.918	42.5
5 radar	73.3	.890	48.7
7 equal	79.8	.919	42.6
7 radar	90.5	.936	37.6
10 equal	96.9	.890	48.2
10 radar	98.9	.927	41.1
13 radar	84.5	.926	41.3

Table 1. Summary fitting results for different zonations. K_{ave} is thickness-weighted average horizontal conductivity, ρ is correlation between observed and predicted drawdown differences, and σ is root-mean-squared scaled residual.

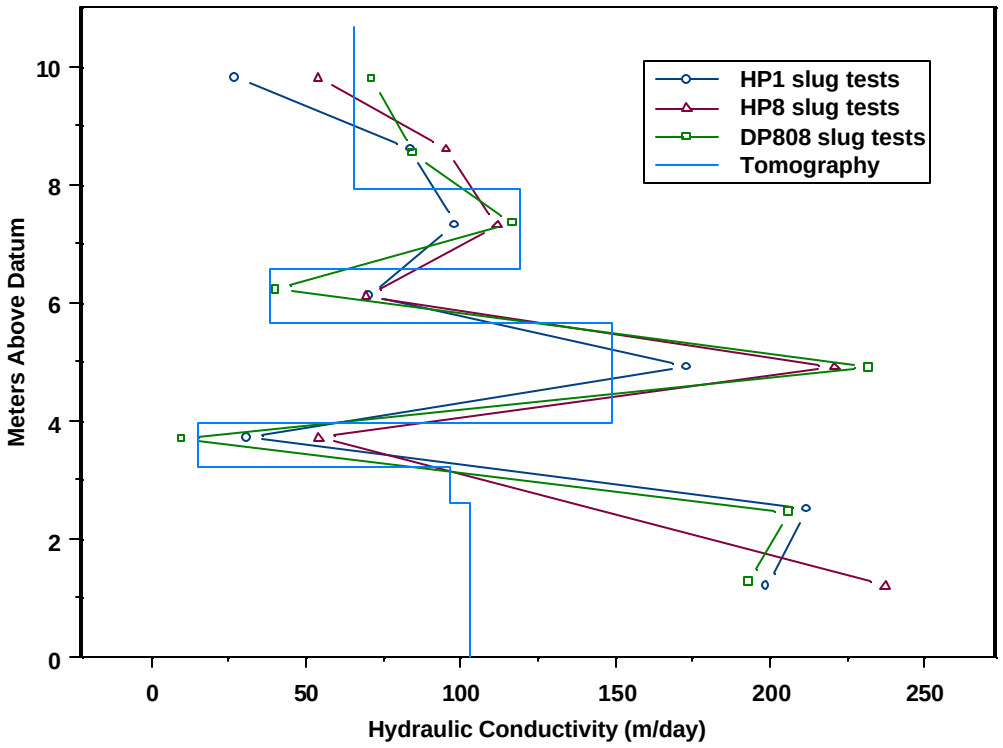

Figure 14. Hydraulic conductivity estimates from hydraulic tomography using 7 radar-based zones compared to nearby direct-push slug test profiles.

Concluding Remarks

The hydraulic conductivity profile estimated using hydraulic tomography with a seven-layer zonation derived from the cross-hole radar survey is presented again in Figure 14, together with the direct-push slug test results. Because of their highly localized nature, direct-push slug tests can be analyzed without regard to questions concerning appropriate aquifer zonation. However, for the same reason, they are fairly insensitive to the lateral extent of the identified high- and low-conductivity zones. Hydraulic tomography, on the other hand, probes a much more laterally extensive region, but the analysis of tomographic pumping tests is sensitive to the selected aquifer zonation. The results of this study demonstrate that electromagnetic and hydraulic property variations in the alluvial aquifer at GEMS seem to be governed to some extent by the same sediment variations, meaning that cross-hole radar surveys show definite promise for providing *a priori* information for flow model zonation. In future work we plan to investigate whether any stronger quantitative relationships can be established between hydraulic and electromagnetic properties at GEMS. We will also work on developing more complicated (laterally varying) aquifer zonations from tomographic radar surveys at the site.

Acknowledgment

This research was supported by the Hydrologic Sciences Program of the National Science Foundation under grant 9903103.

References

Bohling, G.C., and Butler, J.J., Jr., lr2dinv: A finite-difference model for inverse analysis of two-dimensional linear or radial groundwater flow, *Computers & Geosciences*, v. 27, no. 10, pp. 1147-1156, 2001.

Bohling, G.C., Doveton, J.H., Guy, B., Watney, W.L., and Bhattacharya, S., PfEFFER 2.0 Manual, Kansas Geological Survey, 1998.

Bohling, G.C., Zhan, X., Butler, J.J., Jr., and Zheng, L., Steady-shape analysis of tomographic pumping tests for characterization of aquifer heterogeneities, *Water Resources Research*, v. 38, no. 12, 1324, doi:10.1029/2001WRR001176, 2002.

Butler, J.J., Jr., Pumping tests in nonuniform aquifers - the radially symmetric case, Jour. of Hydrology, v. 101, no. 1/4, pp. 15-30, 1988.

Butler, J.J., Jr., Healey, J.M., McCall, G.W., Garnett, E.J., and Loheide, S.P., II, Hydraulic tests with direct-push equipment, *Ground Water*, v. 40, no. 1, pp. 25-36, 2002.

Butler, J.J., Jr., McElwee, C.D., and Bohling, G.C., Pumping tests in networks of multilevel sampling wells: Motivation and methodology, *Water Resources Research*, vol. 35, no. 11, p. 3553-3560, 1999.

Gill, D., Shomrony, A., and Fligelman, H., Numerical zonation of log suites and logfacies recognition by multivariate clustering, *AAPG Bulletin*, v. 77, no. 10, pp. 1781-1791, 1993.

Knoll, M.D., Crosswell radar characterization of the Kansas Geohydrologic Experimental and Monitoring Site: Zero-offset profiles for the Gems4N-Gems4S transect, Progress Report, KUCR Subcontract No. FY2000-063, 2003.

McCall, W., Butler, J.J., Jr., Healey, J.M., Lanier, A.A., Sellwood, S.M., and E.J. Garnett, A dual-tube direct-push method for vertical profiling of hydraulic conductivity in unconsolidated formations, *Environmental & Engineering Geoscience*, v. 8, no. 2, pp. 75-84, 2002.

Parker, R.L., *Geophysical Inverse Theory*, Princeton University Press, 386 pp., 1994.

Schulmeister, M.K., Butler, J.J., Jr., Healey, J.M., Zheng, L., Wysocki, D.A., and G.W. McCall, Direct-push electrical conductivity logging for high-resolution hydrostratigraphic characterization, *Ground Water Monit. and Remed.*, v. 23, no. 3, pp. 52-62, 2003.

Sellwood, S.M., Healey, J.M., Birk, S.M., and J.J. Butler, Jr., Direct-push hydraulic profiling in an unconsolidated alluvial aquifer (abstract), 46th Annual Midwest Ground Water Conference, p. 40, 2001.

Yeh, T.-C. J., and Liu, S., Hydraulic tomography: Development of a new aquifer test method, *Water Resources Research*, v. 36, no. 8, pp. 2095-2105, 2000.